Full Paper Transactions, SMiRT 28
Toronto, Canada, August 10-15, 2025

PRE-DIMENSIONING OF AN EXPERIMENT OF DUCTILE FRACTURE PROPAGATION DUE TO THERMAL SHOCK

Marouane Lahmidi[1], Franck Tankoua[2], Cédric Gourdin[3] and Catherine Gardin[4]

[1] PhD Candidate, CEA Paris-Saclay, Saclay, France (Marouane.lahmidi@cea.fr)
[2] Research Engineer, CEA Paris-Saclay, Saclay, France (Franck.tankoua@cea.fr)
[3] Chief of laboratory, CEA Paris-Saclay, Saclay, France (Cedric.gourdin@cea.fr)
[4] Professor, ISAE ENSMA, Pprime Institute, Chasseneuil, France (Catherine.gardin@ensma.fr)

ABSTRACT

The G_{fr} criterion is a numerical tool to estimate ductile crack propagation. The need is to validate this method in multiple cases of loading. In the case of the thermal shock, ductile crack propagation is unlikely. This makes the experimental validation challenging. To achieve this test, the choice is to combine hot and cold thermal shock, whilst maintaining mechanical effort. Using a first thermomechanical model in Cast3M, an optimized set-up of the experiment is defined. This model was built using temperature independent physical characteristics of the duplex CF8M steel. The convection coefficient and induction penetration depth were fitted on a similar experiment. Concerning the experimental conditions, both heating and cooling systems were specifically set up. The heating system is made up of 3 main components: a monitoring unit, a generator and a cooling system. The cooling system is made to ensure 4-5°C cold water injection in the part, at different flow rates. An unnotched and uncracked hollow CF8M tube is machined for thermal testing. This specimen was drilled with several holes to measure temperature through its length and its thickness, as the thermal gradient is the main enhancer of the crack propagation. The goal of the present work is to compare the simulation and measurements in terms of temperature field. Concerning the thermal gradient on the crack plane, the results were satisfactory. The differences between the measured and estimated temperatures out of the crack plane can be justified by an underestimation of the cooling efficiency, as well as the use of a constant heating power density.

INTRODUCTION

In view of the current projects in the French nuclear sector, the key actors of this field aim to improve the efficiency and accuracy of their numerical predictions. In the area of fracture mechanics, the need is to develop less conservative methods. The G_{fr} criterion is a potential answer to this need, in the case of ductile tearing. Marie (1999) developed this criterion and verified its experimental validity in the case of crack propagation induced by primary stresses. Chapuliot et al. (2020) adapted the G_{fr} criterion to the case of secondary stresses, especially thermal shocks. The aim of this work is to evaluate experimentally the validity of the G_{fr} criterion in this specific case, in addition to studying the criticality of thermal shocks on high-thickness components in the nuclear industry.

Ductile tearing due to thermal shock is an unlikely failure mode for thick components, which makes more difficult its experimental reproduction. Nevertheless, this kind of experiments was carried out in the frame of the FALSIRE project (Fracture Analyses of Large-Scale International Reference Experiments) organized by the Committee on the Safety of Nuclear Installations (1996). The objective of this project was to compare

several fracture calculation methods through the analysis of large-scale tests. These tests are a combination of mechanical and thermal loadings referred to as PTS (Pressurized Thermal Shock). These combined loadings replicate the stresses that occur in the pressurized pipes of nuclear reactors following incidents of coolant loss. PTS conditions can be applied in different ways. For some of these experiments, a heated pipe was pressurized, and the thermal shock was induced by injecting coolant either inside (Bethmont et al. (1990)) or outside (Bryan et al. (1989) and Keinänen et al. (1995)). In these experiments, the ductile crack propagation exceeded 3 mm.

In the experiment of Morland et al. (1992), a thick tube with a crack on its inner surface is heated, then cooled by injecting cold water onto the surface while rotating the tube around its axis using a dedicated device. The STEP test (Okamura et al. (1992)) consists of a plate with a surface crack subjected to mechanical bending and tensile loadings, as well as a thermal shock on the cracked surface. In these experiments, the ductile crack propagation did not exceed 1mm.

The following experiments are applied on high thickness specimens: 200mm for Bethmont et al. (1990) and Morland et al. (1992), 150mm for Bryan et al. (1989) and Keinänen et al. (1995), 170mm for Okamura et al. (1992).

In the Laboratory of Structural Integrity and Normalization of the Atomic Energy Center, we are developing an innovative experiment that combines, in a simultaneous way, mechanical tension loading, hot thermal shock by induction heating and cold thermal shock by water-cooling. The test specimen is less massive compared to the mentioned experiments. This improves the reproducibility of the test and reduces costs, whilst maintaining a considerable ductile crack propagation. This experiment is based on a thermal fatigue experiment called PROFATH (Gourdin et al. (2018)), developed in the same laboratory. The PROFATH test involves alternately heating and cooling a tube in order to propagate a crack through thermal fatigue. One of the initial steps in order to elaborate our new experiment is the pre-dimensioning and the thermal testing. This document presents work carried out within this context.

PRE-DIMENSIONING OF THE THERMAL SHOCK EXPERIMENT

The goal of this part is to determine an optimal configuration of the experiment to maximize ductile crack propagation.

Steps of the thermal shock crack propagation experiment

The specimen of the experiment is a hollow tube with a circumferential crack. The tube is heated on its external surface using an inductor, and it is cooled on its internal surface with cold streaming water. At the beginning of the experiment, the specimen is heated at 200°C. Then, the thermal shock is created by simultaneously heating the external surface through induction at 400°C, and cooling the internal surface with streaming water at a temperature of 4-5°C. This procedure has two main advantages. Firstly, the thermal gradient through the thickness is high and maintained. It maximizes the secondary stresses, and therefore the efficiency of the experiment. Secondly, the crack tip temperature during the propagation stays in the range of 150°C-250°C. This facilitates the simulation of the ductile fracture with the G_{fr} criterion and keeps the tenacity of the material low.

Material characteristics

The specimen is composed of CF8M. It is a duplex austenoferritic steel, that has a very low tenacity when it is aged to a temperature of 400°C. The Table 1 gives the values of various material characteristics that

will be used to pre-dimension the specimen. It is considered that the properties in Table 1 do not vary with temperature.

The Equation (1) is a power law that represents the behaviour of the CF8M:

$$\begin{cases} \sigma = \sigma_y + B_1.{\varepsilon_p}^{A_1} \left(0 < \varepsilon_p < 0.009\right) \\ \sigma = \sigma_y + B_2.{\varepsilon_p}^{B_2} \left(0.009 < \varepsilon_p\right) \end{cases} \quad (1)$$

Where σ is the tensile stress, ε_p is the plastic strain, $\sigma_y = 236\ MPa$ is the yield strength.
$B_1 = 3163\ MPa$, $B_2 = 1031\ MPa$, $A_1 = 0.46$, and $A_2 = 0.24$ are parameters of the power law.

Table 1: Thermal and mechanical characteristics of the CF8M steel.

Thermal conductivity $[W.°C^{-1}.m^{-1}]$	16.6
Thermal capacity $[J.°C^{-1}.kg^{-1}]$	550
Mass density [kg/m^3]	7800
Young modulus [GPa]	184
Expansion coefficient $[°C^{-1}]$	16.6×10^{-6}
Crack initiation tenacity J_{IC} $[kJ/m^2]$	40
Crack propagation tenacity [MPa]	35

Finite element conditions

The used bidimensional mesh is meant to represent the tube's longitudinal section. The model is thermoelastoplastic and axisymmetric. The mesh is refined and partitioned near the crack to enable the use of the G-THETA procedure. As described in the Figure 1, only the superior part of the specimen is meshed since the model is symmetric in both sides of the crack plane. Therefore, the elements representing the cracked ligament are blocked along the z direction. The length of this part is equal to l_{tot} .

A tensile load is applied on the upper elements of the mesh. The value of the mechanical loading is chosen such as the J-integral is equal to the crack initiation tenacity. The J–integral is calculated using the G-THETA procedure in Cast3M. Therefore, the mechanical loading will depend of the crack length l_{fiss}. The thermal boundary conditions are represented in the Figure 1. A temperature of 20°C is imposed on the upper elements of the mesh. Moreover, a portion of the internal surface (height l_{co}), in the vicinity of the symmetry plane, is subjected to a convection condition with a water temperature of 5°C. A portion of the external volume of the tube is also subjected to a heating power density. The heating power density is spatially constant in the red zone (height l_{ind}) in the Figure 1, and it is calculated numerically to match a desired value of the temperature at the point H.

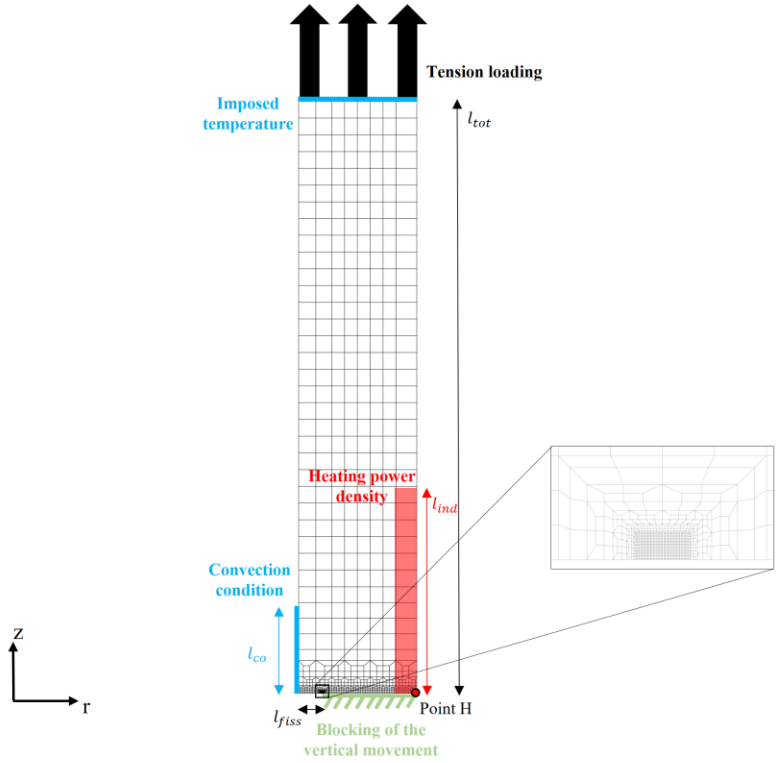

Figure 1. Mesh and elements of the thermoelastoplastic model

The calculation is divided to 3 steps. The first step corresponds to the thermal heating. As described in the Figure 2.a, the heating increases the temperature at the point H (on the external surface, on the crack plane (z=0)) to 200°C progressively for a duration of 1 hour. The second step is that of mechanical loading. The applied load increases linearly as described in the Figure 2.b. The third step consists in the thermal shock, which combines an instantaneous rise of the convection coefficient from 25 $W.°C^{-1}.m^{-2}$ to 3500 $W.°C^{-1}.m^{-2}$. These values were fitted using the results of a similar thermal fatigue experiment, as well as the thickness of the heating zone (Gourdin et al. (2018)). This rise of the convection coefficient is combined with a rise of the monitored temperature from 200°C to 400°C.

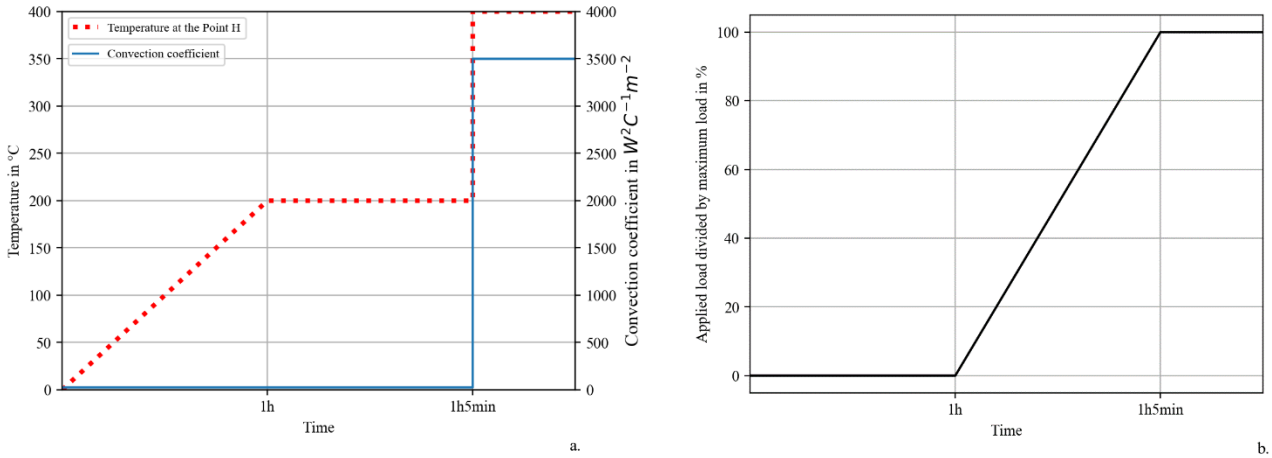

Figure 2.a) Evolution of thermal quantities during calculation.
b) Evolution of tension loading during calculation

The goal is to find the optimum values, whilst considering machining requirements, of the quantities l_{co}, l_{fiss}, l_{ind} et l_{tot}, represented in the Figure 2. The realized optimization concluded that the optimal values were $l_{co} = 18\,mm$, $l_{fiss} = 4\,mm$, $l_{ind} = 75\,mm$ et $l_{tot} = 100\,mm$.

The Figure 3 represents the resulting temperature field and the deformed mesh at three different instants, before and after the thermal shock. The amplification of the deformed mesh is equal to 20. As expected, the simultaneous cold and hot thermal shock creates a high thermal gradient throughout the thickness. This thermal gradient is causing a contraction of the inner surface combined with a swelling of the external one. This structural effect is meant to enhance the crack propagation. The cold zone is localized around the crack tip. As $l_{co} < l_{ind}$, a zone with a temperature higher than 400°C appears above the crack plane. At 50 seconds after the thermal shock, the temperature exceeds 450°C in this zone. For CF8M steel, the creep becomes considerable at such a temperature. Since the propagation of the crack is almost finished at this instant, it hasn't been necessary to add a creep model.

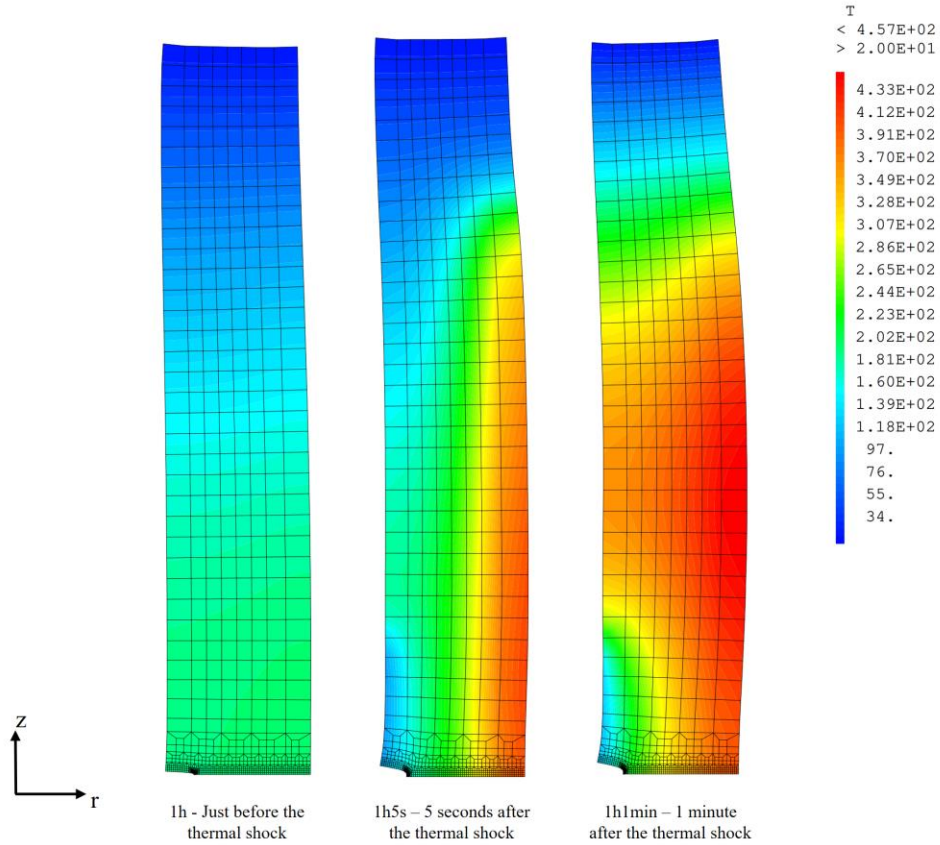

Figure 3. Temperature field and deformed mesh of the optimized model

EXPERIMENTAL PROCEDURE

Experiment measurement of the temperatures

For this study, with aims of thermal testing without mechanical loading, a specific specimen was designed. This tube has an internal diameter of 39 mm and a thickness of 21 mm. The length is 280 mm, with a 50 mm long thread at each end. The tube is unnotched and uncracked.
To measure the temperature, Type K basic thermocouples were used. A total of 33 holes were machined to place thermocouples through the thickness of the specimen (Figure 4). The thermocouples were placed symmetrically at 6 different distances along z from the symmetry plane (respectively 0, 9, 18, 27, 41, 54 mm). At each of these 11 positions along z, 3 holes were machined along the circumference at depths of 18.5mm, 16.5mm and 14.5mm. In addition to the 33 thermocouples placed through the depth of the specimen, 33 other thermocouples were welded on the external surface of the specimen: 3 thermocouples were welded on each of the 11 planes of the specimen. These 3 thermocouples are equidistant with an angle of 120° as shown in the Figure 4.

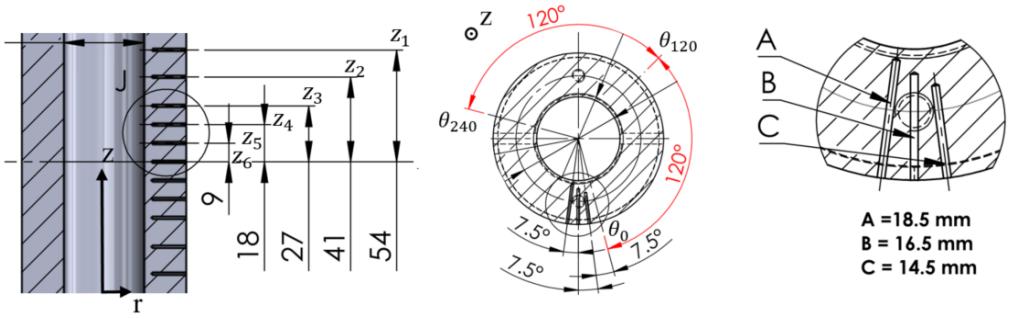

Figure 4. Positions of the different type K thermocouples

The heating is realised using an inductor with a power of 12kW. The induction device is composed of a monitoring unit, a generator and a cooling system. The heating power is monitored by the thermocouple that corresponds to the Point H in the Figure 1. The monitoring thermocouple is welded on the external surface, on the crack plane (z=0) and near the machined holes (Measurement line θ_0). Therefore, the induction monitoring unit regulates the heating power to obtain a good fitting between the thermocouple indication and the required temperature evolution. The induction coil showed in the Figure 5.a is 150mm long with an internal diameter of 110mm and 10 turns.

Figure 5.a) Thermal testing experiment, with induction heating system, and connections of all the thermocouples. b) Injector

The cooling of the specimen is realised by injecting 4-5°C water inside of the testing tube. The water is cooled using an Air-cooled liquid chiller with a 4.67 kW power. This device is connected to a 1000 liters water tank. Once the water is cooled, it is injected from the tank to the specimen with a pump. Using a control valve, the flow can vary between 71 cm^3/s and 178 cm^3/s. The circulation of the water in the specimen is done through two similar parts represented in the Figure 5.b. The two parts are threaded into the specimen on both ends. The goal is to localize the cooling of the specimen near the crack. The design is made so that the water is in direct contact with the specimen over a length of $2l_{co}$ = 36mm.

The thermal testing is divided to 3 steps, as in the previous FEM approach: First, the specimen is slowly heated to a temperature of 200°C for a duration of 1 hour. The heating is monitored with a thermocouple welded on the external surface, on the crack plane, in order to reach the value of 200°C at the end of this first heating phase. During this phase, the position of the coil is modified in order to make sure that the temperature field in the specimen is symmetric on both sides of the crack plane and axisymmetric. During the second phase, the temperature on the monitored thermocouple is maintained at 200°C for 5 minutes. During the last phase, the induction power is suddenly increased in order to reach a temperature of 400°C, which induces a hot thermal shock. At the same time, the cold water is injected in the specimen, inducing a simultaneous cold thermal shock.

This procedure is repeated several times and a correct reproducibility is observed. The measurements at different angles (θ_0, θ_{120}, θ_{240}) are compared. A good agreement is found between these measurements at different heights z_i, indicating that the temperature field can be considered axisymmetric.

COMPARISON SIMULATION – EXPERIMENT

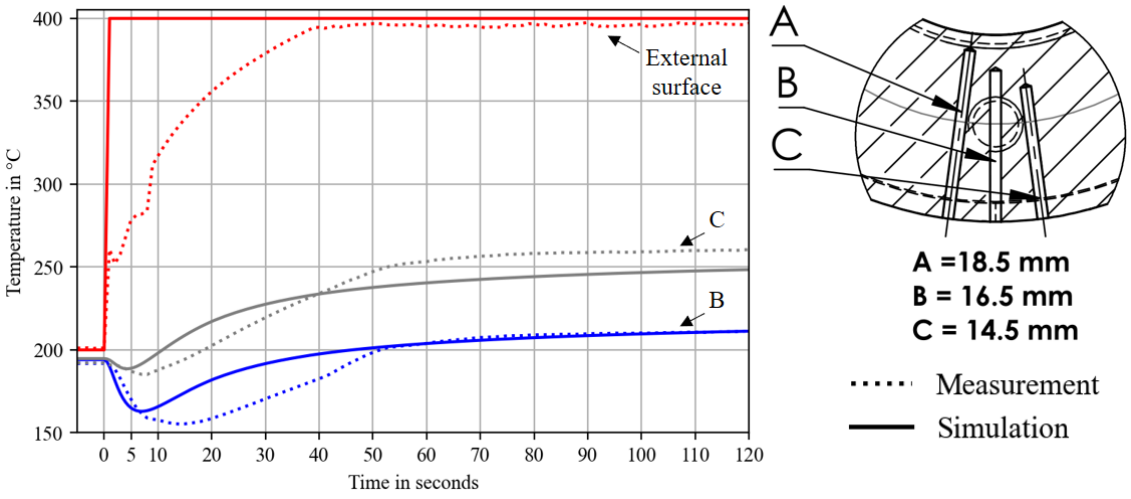

Figure 6. Evolution of estimated and measured temperatures on the crack plane

The Figure 6 allows to compare the experimental and predicted temperature at the external surface and the depths B, C. Because of experimental issues, the measures in depth A were not properly recorded. The instant 0 corresponds to the initiation of the thermal shock. The accuracy between measurement and simulation values before the instant 0 indicates that the heating phase is well reproduced.
As mentioned in the Experimental procedure and Simulation paragraphs, the heating is monitored by the temperature on the point at the intersection of the crack plane and the external surface. Despite an induction power of 12 kW, 40 seconds are necessary to reach the instruction and the simulation. It is partly due to the

simultaneous cooling of the specimen and the limited power of the inductor. This gap causes a latency compared to the simulation.

Inside the specimen, at the position of thermocouples B and C, a first decrease of the temperature, due to the cold thermal shock is noticed. It represents the thermal transient caused by the cooling. The simulation correctly reproduces this phase. As B is closer to the internal cooled surface, the decrease is consequently more important in this position.

This initial decrease is followed by a second step of temperature increase, due the external hot shock. A quasi permanent state is obtained after approximately 50 seconds in the whole thickness of the tube. The corresponding value is higher near the external surface.

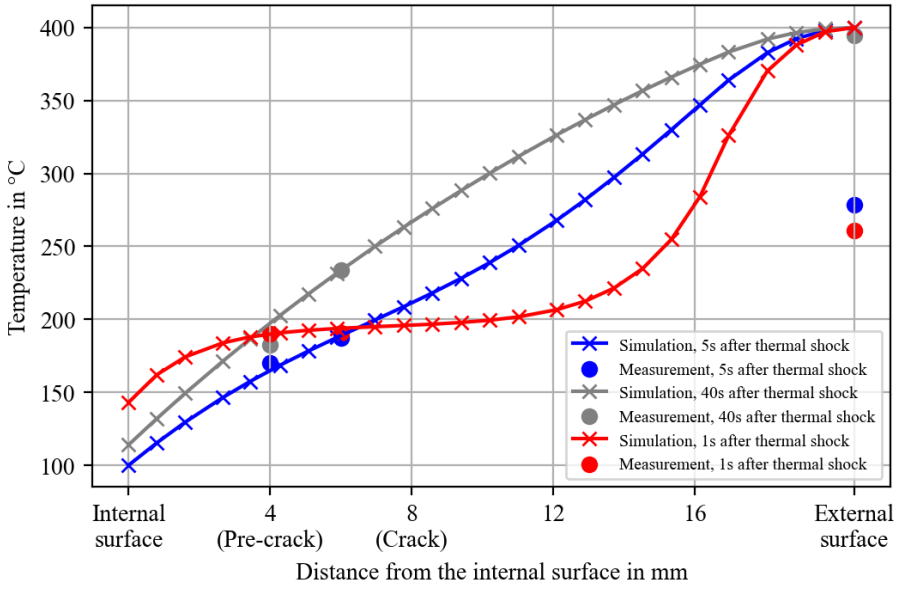

Figure 7. Variation of the temperature throughout the thickness on the crack plane

Concerning the measurements and calculation of the temperature on the crack plane, a good agreement is found. This indicates that the convection value of 3500 $W.°C^{-1}.m^{-2}$. fitted on the PROFATH experiment, is adapted. The Figure 7 represents the temperature changes inside the thickness of the tube at different times (1, 5, 40 seconds) after the thermal shock, on the crack plane. Only 3 thermocouples were positioned in the thickness, whereas predictions are available throughout the thickness. This figure confirms this good agreement between experiments and predictions, despite the gap on the external surface.

Considering an initial 4 mm internal pre-crack leading to 4 mm ductile crack propagation, the Figure 7 demonstrates that, 5 seconds after the thermal shock, the crack tip temperature varies between 165°C and 215°C. No significant evolution of the fracture toughness is expected for such temperature variation. This result aligns with our aim to maintain consistent toughness characteristics at the crack tip.

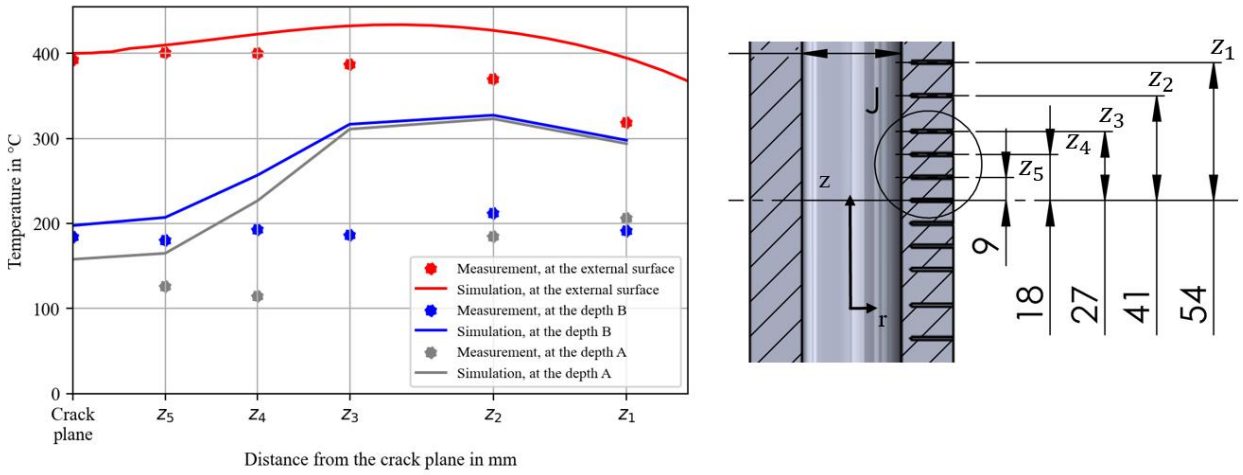

Figure 8. Variation of the temperature throughout the length z, 40 seconds after the thermal shock

Out of the crack plane, the model overestimates the measured temperatures, as illustrated in Figure 8, 40 seconds after the thermal shock. The hot zone described in the pre-dimensioning analysis appears on the external surface with a maximum temperature of 425°C, whereas this phenomenon isn't experimentally observed. This gap suggests that the heating power density in the model should be improved. The first step would be to change the quantity l_{ind}. It is also considered to implement a smoother variation of the heating density in space, using exponential, hyperbolic or Bessel functions (Develey(2000)). In addition to that, the evolution of the monitored temperature will be modified to match with the measured evolution. Also, the two other discrepant curves in the Figure 8 correspond to 18.5mm and 16.5mm deep measurements. Their closeness to the internal surface indicates that they are more influenced by convection parameters. Therefore, the convection model should be improved. As described in the Figure 1, the convection condition is applied exclusively on a zone with a length of l_{co}. In reality, the streaming water is injected throughout the part in the Figure 5.b. And this part is threaded with the specimen. Consequently, the specimen might be cooled through contact with the injector. To improve the cooling model, it is proposed to add a mesh representing the injector, as well as a thermal resistance model to simulate the heat exchange due to the contact between the specimen and the injector.

CONCLUSION

In order to develop the thermal shock experiment, a pre-dimensioning study was carried out. The goal was to identify the optimal parameters and dimensions of the experiment. Therefore, a thermoelastoplastic and axisymmetric model of the experiment was built using CF8M material characteristics and the software Cast3M. Based on the optimal configuration determined by the pre-dimensioning, the thermal testing was set up. A specific tube was machined with holes that allow temperature measurement throughout the thickness. Moreover, specific induction heating and water-cooling systems were installed. The analogy between the optimized model and the thermal testing proved right to model the thermal behaviour at the crack plane. Nevertheless, it demonstrates certain discrepancies (absence of an overheating zone, underestimation of the cooling). This comparison provides hints to improve the numerical model, in order to obtain a more reliable estimation of the temperature field in the whole part, and thus of the crack propagation.

ACKNOWLEDGMENTS

The authors warmly thank Chléa Leliévre, Thierry Legrasse, Julien Leroy and Ivan Tournié for their work and contribution to building this experiment.

REFERENCES

Bethmont, M., Rousselier, G., Kussmaul, K., Sauter, A. and Jovanovic, A. (1990) "The method of "local approach of fracture" and its application to a thermal shock experiment," *Nuclear Engineering and Design*, 119(2) :249–261.

Bryan, R. H., Bass, B. R., Bolt, S. E., Bryson, J. W., Corwin, W. R., Nanstad, R. K., Merkle, J. G. and Robinson, G. C. (1989) "Performance of low-upper-shelf material under pressurized-thermal-shock loading," *Nuclear Engineering and Design*, 115(2) :359–367.

Chapuliot, S., Ancelet, O. and Marie, S. (2020). "Assessment of the defect stability for large structures submitted to thermal shock loading through the G_{fr} criterion," *International Journal of Pressure Vessels and Piping*, 182 (2020), 104066.

Committee on the Safety of Nuclear Installations. (1996). "FALSIRE PHASE II: CSNI Project for Fracture Analyses of Large-Scale International Reference Experiments," *Technical Report NEA/CSNI/R(96)1*, OECD Nuclear Energy Agency, France.

Develey, G. (2000). "Chauffage par induction électromagnétique: principes", *Énergies | Réseaux électriques et applications*, Techniques de l'ingénieur, Quelques rappels théoriques, 4-12

Keinänen, H., Talja, H., Rintamaa, R., Törrönen, K., Ahlstrand, R., Nurkkala, P., Karzov, G., Timofeev, B. and Blumin, A. (1995). "Crack initiation and arrest in a pressurized thermal shock test for a model pressure vessel made of VVER-440 reactor pressure vessel steel," *Nuclear Engineering and Design*, 158(2) :217–226.

Gourdin, C., Perez, G., Le Delliou, P., and Leopold, G. (2018). "Investigations on crack propagation under cyclic Iisothermal and thermo-mechanical loadings for A Type 304-L stainless steel used for pressurized water reactor," *12th International Fatigue Congress,* MATEC Web Conference, Volume 165, Number 19004

Marie, S. (1999). "Approche énergétique de la déchirure ductile", PhD thesis, Atomic Energy Commission, Ecole Nationale Supérieure de Mécanique et d'Aéronautique et Faculté des Sciences Fondamentales et Appliquées, Saclay, France.

Morland and Sherry A. H. (1992). "Spinning Cylinder Experiments SC-I and SC-Il : A review of results and analyses provided to the FALSIRE Project," AEA Technology, Reactor Services, United Kingdom.

Okamura, H., Yagawa, G., Kawakami, T., Urabe, Y., Sato, M. and Sano. J. (1992). "Ductile crack growth under a PTS event," *Nuclear Engineering and Design*, 137(3) :457–465.